ISSN 0016-7029, Geochemistry International, 2006, Vol. 44, No. 1, pp. 33–47. © Pleiades Publishing, Inc., 2006.
Original Russian Text © A.A. Kadik, Yu.A. Litvin, V.V. Koltashev, E.B. Kryukova, V.G. Plotnichenko, 2006, published in Geokhimiya, 2006, No. 1, pp. 38–53.

Solubility of Hydrogen and Carbon in Reduced Magmas of the Early Earth's Mantle

A. A. Kadik*, Yu. A. Litvin, V. V. Koltashev***, E. B. Kryukova***, and V. G. Plotnichenko*****

**Vernadsky Institute of Geochemistry and Analytical Chemistry, Russian Academy of Sciences, ul. Kosygina 19, Moscow, 119991 Russia*
e-mail: kadik@geokhi.ru
***Institute of Experimental Mineralogy, Russian Academy of Sciences, Chernogolovka, Moscow oblast, 142432 Russia*
****Research Center for Fiber Optics, Institute of General Physics, Russian Academy of Sciences, ul. Vavilova 38, 119991 Russia*

Received February 1, 2005

Abstract—The solubility of volatile compounds in magmas and the redox state of their mantle source are the main factors that control the transfer of volatile components from the planet's interior to its surface. In theories of the formation of the Earth, the composition of gases extracted by primary planetary magmas is accounted for by the large-scale melting of the early mantle in the presence of the metallic Fe phase [1, 2]. The fused metallic Fe phase and the melted silicate material experienced gravitational migration that exerted influence upon the formation of the metallic core of the planet. The large-scale melting of the early Earth should have been accompanied by the formation of volatile compounds, whose composition was controlled by the interaction of H and C with silicate and metallic melts, a process that remains largely unknown as of yet.

DOI: 10.1134/S0016702906010058

INTRODUCTION

A series of experiments in the system Fe-bearing melt + fused metallic Fe phase (0.1–7% Si) + C (graphite) + H_2 at 4 GPa and 1550–1600°C allowed the characterization of the nature of H and C compounds dissolved in silicate melts. The infrared and Raman spectroscopic measurements of the glasses as products of quenching of reduced melts were used to elucidate the mechanisms of H and C dissolution.

The study of the stability of the metallic Fe–Si phase at a pressure corresponding to a depth of 100–150 km has shown that its melting results in the formation of silicate liquids that contain both oxidized and reduced H and C species. The relationships between them substantially depend on fO_2. At $\Delta\log fO_2(IW) = -(2.0–2.5)$, hydrogen occurs in the melt largely as the OH^- group and H_2O. Some amount of hydrogen is dissolved in the molecular form. Carbon is soluble mainly in the atomic form, as insignificant quantities of the carbonate ion CO_3^{2-}, and as carbon bound in the melt with Si (bond of the Si–C type). Thereby, the melts are characterized by the preferential dissolution of H in comparison with C. At lower $\Delta\log fO_2(IW)$ values of –(4–6) and in the presence of the liquid Fe–Si phase, the character of H and C dissolution markedly changes. The H solubility as OH^- decreases, while the H solubility as H_2 increases. The C solubility in the melt is related to the formation of the C–H bond that corresponds to CH_4. As fO_2 falls, the amount of dissolved H (recalculated to water) decreases from 1.6–1.8 wt % H_2O at $\Delta\log fO_2(IW) = -2.3$ to 0.8–1.0 wt % at $\Delta\log fO_2(IW) = -5.7$. At the same time, the C solubility increases from 0.2 wt % at $\Delta\log fO_2(IW) = -2.3$ to ~2 wt % at $\Delta\log fO_2(IW) = -5.7$.

The experimental results lead to the conclusion that the proportions of reduced and oxidized species of carbon in the primary melts substantially depend on the fO_2 of the reduced mantle. At $\Delta\log fO_2(IW) \approx -2$, which corresponds to the equilibrium of Fe with olivine in the upper mantle, oxidized H species are prevalent in the melt equilibrated with metallic Fe. If the chemical fractionation of the early mantle occurred at lower fO_2 values at $\Delta\log fO_2(IW) = -(3–5)$, which are expected for the enstatite-chondrite model of the mantle formation [3], then the compounds with C–H-type bonds (CH_4 and other molecules with such a bond) should be expected in the primary melt, together with oxidized H species (OH^- group). These volatile H and C compounds are associated with the formation of a liquid Fe phase enriched in Si. The oxygen fugacity during the formation of the magmatic ocean is of principal importance for the estimation of the gas composition with respect to H_2O, H_2, and CH_4 extracted from the reduced planetary matter and supplied to the surface in the course of high-temperature volcanic activity.

FORMULATION OF THE PROBLEM

The origin and evolution of volatile components in the Earth remain ambiguous in many respects (see, for

example, [4]). A number of models describe the composition of volatile components deduced from the data on the solar system during and soon after the accretion. In particular, it is suggested that the primary contents of H_2O and rare gases were controlled by the participation of H-bearing planetesimals in accretion [4, 5]. Another point of view is based on the assumption that solar gases enriched in hydrogen participated in accretion [6]. According to [7], the homogeneous accretion of the Earth was characterized by the formation of an outer shell consisting of late carbonaceous chondrites enriched in volatiles.

The study of isotopic and elemental compositions of rare gases indicates that, despite the intense degassing of accreted matter affected by impact processes, part of the volatile components has been buried in the solid silicate mantle [8]. According to [3], oxygen and carbon were contained in the solid silicate mantle during or after the main events related to the segregation of the metallic core. In light of these data, H and C compounds that occurred in the early mantle could have served as an internal source of volatile components.

The degassing of the accreted material as a result of impact processes that gave rise to the substantial heating and melting of deep-seated matter and to the formation of a magmatic ocean is considered the main cause of the transfer of volatile components from the planet's interior, a process that gave rise to the formation of the early terrestrial atmosphere [9, 10]. The proportions of the reduced (CH_4, H_2, CO) and oxidized (H_2O, CO_2) hydrogen and carbon species that were supplied into the upper shells of the Earth remain a matter of debate. A reduced atmosphere enriched in CH_4 is regarded as a prerequisite for the prebiological evolution of organic matter that eventually led to the origin of life on the Earth's surface [11].

The gas regime of the early Earth with respect to the contents of oxidized and reduced H and C species was closely related to the redox state of the planetary matter, its dependence on the chemical differentiation of the mantle and the conditions of metallic core formation, as well as on the specific features of the dissolution of volatile components in the products of the early melting [12].

The study of phase equilibria as a tool for the measurements of oxygen fugacity shows that the present-day lithospheric and asthenospheric layers are oxidized to a moderate extent, and the respective fO_2 values are above the equilibrium with the metallic Fe phase. The Fe^{3+} activity in minerals from the upper mantle fits the fO_2 values that determine the prevalence of CO_2 and H_2O in deep fluids and the stability of carbonate phases.

Nevertheless, the idea about the reduced state of the Earth's mantle controlled by chemical equilibrium with the metallic Fe phase and the metallic core at the early stage of Earth formation also has certain grounds [13–20]. If the mean olivine composition in the upper mantle is accepted to be Fo_{91}, then fO_2 should be at least two logarithmic units lower than the fO_2 of the Fe–FeO equilibrium at IW buffer ($\Delta\log fO_2(IW) = -2$) or at least six logarithmic units lower than the fO_2 of the lithospheric and asthenospheric layers of the modern upper mantle. At this redox state of the planetary matter, CH_4 and H_2 in equilibrium with free carbon (graphite or diamond) should be the predominant volatile components. The early mantle was probably characterized by a lower fO_2 than that following from equilibrium between Fe and Fo_{91}. According to Javoy's model [3, 21, 22], which assumes the participation of enstatite chondrites in the formation of the Earth, the early mantle might have been reduced, with $\Delta\log fO_2(IW)$ varying from –3 to –5. Such a mantle could not have contained water, so that reduced H and C species and free carbon should be the prevalent volatiles.

The causes that gave rise to the oxidation of the primordial mantle matter and brought about the change in the fluid composition remain obscure in many respects. It cannot be ruled out that the oxygen potential in the mantle was gradually increasing, beginning in the early Archean, due to the hydrogen dissipation, processes of recycling [16, 18, 20, 23], or the addition of the "oxidized" material of carbonaceous chondrites at a later stage of accretion [3, 21, 24]. Some authors recently put forth the idea of oxygen release as a result of mantle interaction with the metallic core and the corresponding oxidation of the mantle [3, 19, 25].

Physical theories of the genesis of the early Earth's mantle suggest the large-scale melting of the mantle with the origin of a magmatic ocean that exerted influence upon chemical differentiation [1]. The melting proceeded in the presence of a metallic Fe phase [2] and, thus, at a low fO_2. The properties of reduced magmas equilibrated with Fe and its alloys remain ambiguous in many respects, in particular, as concerns the dissolution of volatile components in silicate liquids. However, the available experimental results on the interaction of CH_4, H_2, and elementary C with silicate melts revealed an important feature of redox reactions in silicate melts [12, 15, 26–29]. It turns out that, even when the oxygen fugacity is below the IW buffer equilibrium, oxidized hydrogen and carbon species (H_2O, OH^-, CO_3^{2-}) are stable. This feature of CH_4, H_2, and C interaction with silicate melts may be crucial for the elucidation of the mechanisms of CO_2 and H_2O formation in the course of magma generation in the reduced mantle in which these compounds are instable. Experiments in the system Fe-bearing melt (ferrobasalt) + liquid metallic phase Fe + H_2 + C (graphite) at 3.7 GPa, 1520–1600°C and $\Delta\log fO_2(IW) = -2.4$ lead us to suggest that the magmas derived from the reduced C-bearing planetary mantle may contain more oxidized C and H species that the mantle source itself [12]. From this point of view, the melting of the reduced mantle might

be a possible mechanism of the H_2O and CO_2 formation in the geologic past and the transfer of these volatiles to the surface.

However, many specific features of C and H dissolution in the reduced melts remain unclear. In particular, this concerns the effect of fO_2 on the proportion of "oxidized" (H_2O, OH^-, CO_2, CO_3^{2-}) and "reduced" (H_2, CH_4, SiC, C) species in melts that might determine the formation of the early magmatic melts with high CH_4 and H_2 contents. In this work, continuing the previous investigations [12], we carried out experiments on the equilibrium of Fe-bearing melt (ferrobasalt) + liquid Fe phase + H_2 + C (graphite) at 4 GPa, 1520–1600°C and $\Delta\log fO_2(IW) = -(3–6)$. The silicate component of this system is regarded as a model one, and its reduction with the formation of metallic Fe phase provides insights into the redox reactions in magmatic liquids in the presence of H and C. The choice of low fO_2 values for runs was based on available information on the primordial redox state of the mantle matter in terms of the chondrite and enstatite-chondrite models of the Earth's formation [3, 25]. To elucidate the mechanisms of H and C dissolution, infrared and Raman spectroscopy were applied to the glasses produced by the quenching of the reduced melts.

HIGH-PRESSURE EXPERIMENTS

The experiment was performed on an anvil-type apparatus at 4 GPa and 1550–1600°C under a controlled hydrogen fugacity [12, 30]. The space inside the heater was 6 cm^3 and was characterized by temperature and pressure variations within the limits of ±5°C and ±0.1 GPa, respectively. A sample was placed into the sealed Pt ampoule 10 mm in diameter and 5 mm in height. The temperature was measured with a Pt30%Rh/Pt6%Rh thermocouple mounted radially at the cell center between two capsules. The accuracy of temperature measurements was ±5°C at 1500°C and close to ±10°C at 1600°C. The pressure at a high temperature was calibrated on the basis of the quartz–coesite transition [31]. The reproducibility of pressure in the runs is estimated at ±0.1 GPa.

As in the previous experiments [12], the silicate component of the mixture was prepared from natural ferrobasalt (wt %): Na_2O (2.68), MgO (4.98), Al_2O_3 (13.12), SiO_2 (49.18), K_2O (0.36), CaO (8.40), TiO_2 (1.95), MnO (0.28), FeO (18.01), and P_2O_5 (0.22). The starting material was a powder of glass prepared by melting in an alundum crucible at 1250°C in the presence of N_2 and then quenched into colorless glass. Its composition and homogeneity were verified with microprobe analyses. To create a low fO_2 in the experiments, 5 and 10 wt % of finely dispersed SiC was added to the glass powder. The weight of the mixture was 200–300 mg. A graphite disc 0.2 mm in thickness was placed above the sample (Fig. 1). The sample was isolated from the walls of the Pt ampoule with a tungsten foil 0.05 mm thick to eliminate interaction between the Fe-bearing melt and Pt [30]. The runs lasted 30–60 min. The run products were quenched by switching off power to the heater. The initial rate of quenching was ~200°C/s.

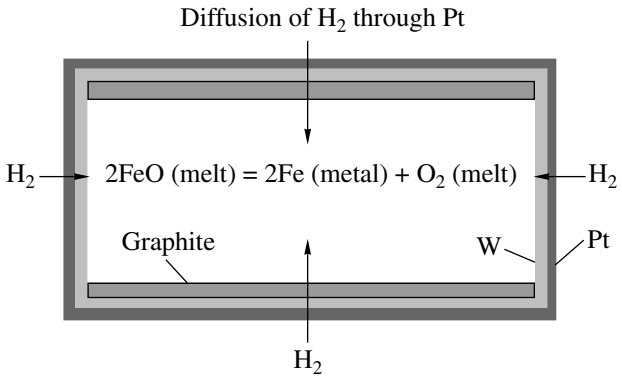

Fig. 1. Experimental conditions at a low fO_2 including the following stages [12]: (1) diffusion of H_2 into the platinum capsule from the outer assemblage of apparatus; (2) formation of a metallic Fe phase with the release of O_2; and (3) interaction of H and O with melt and graphite, formation of "oxidized" and "reduced" hydrogen and carbon compounds in silicate liquid.

HYDROGEN AND OXYGEN FUGACITY

The fO_2 buffering used in the experiment was based on H_2 diffusion through Pt with the achievement of an equal chemical potential of H_2 inside and outside the Pt ampoule in the solid assemblage of the apparatus that controls buffering fH_2 in the presence of H_2O traces. Ulmer and Luth [32] applied this method to study equilibrium in the system graphite–C–O–H fluid. In our case, fH_2 was buffered by the assemblage of the heater at the fO_2 values that maintain the Fe–FeO (IW) equilibrium [12]. At a given temperature, pressure, and fO_2, the fH_2O/fH_2 ratio in the O–H system outside the capsule acquires a constant value. Inside the platinum capsule, the fO_2 values are controlled by the equilibrium between graphite, H_2 buffered from outside, and components of silicate melt that are reduced with the release of oxygen and the formation of metallic Fe (Fig. 1).

Calculations for C–O–H system demonstrate that, at a given fH_2, the fO_2 value at equilibrium of graphite with a C–O–H fluid inside the platinum capsule must be much lower than in the O–H fluid phase outside the latter (Fig. 2). Precisely these relationships are used to attain a low fO_2 value in experiments. Our experiments were carried out in the absence of a free C–O–H phase within the Pt capsule, as was proved by the microscopic and spectral examination of quenched glass. In the presence of a free fluid phase during the runs, CH_4 would be the prevalent component (Fig. 3).

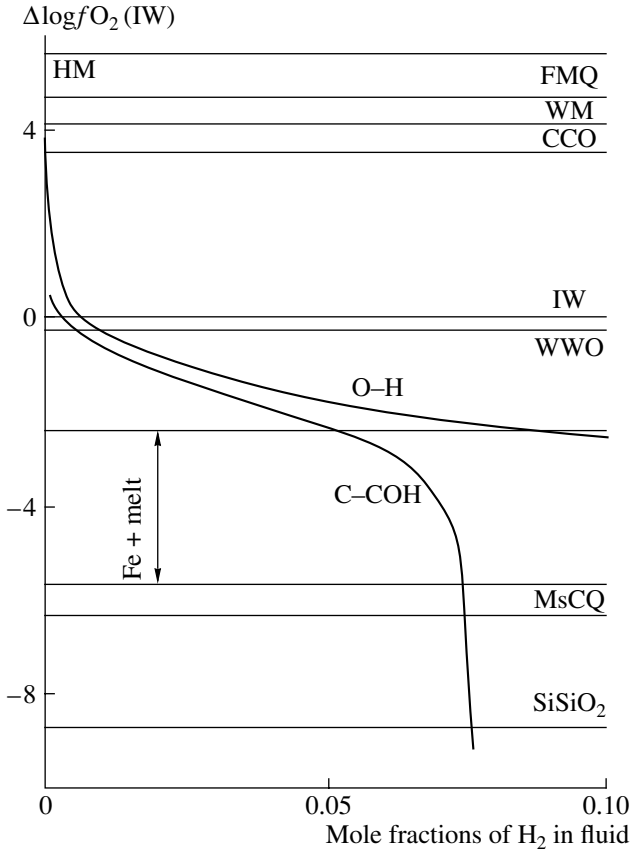

Fig. 2. fO_2 (relative to IW buffer) of C–O–H fluid in equilibrium with graphite versus mole fraction of H_2 in fluid. Location of oxygen buffers: Fe_2SiO_4–Fe_3O_4–SiO_2 (FMQ), FeO–Fe_3O_4 (WM), Fe–FeO (IW), after [33]; SiC–C–SiO_2 (MsCQ), after [34]; Si–SiO_2 (SiSiO$_2$), after [26]. Reaction $C + O_2 = CO_2$ (CCO) determines the upper limit of graphite stability. The fO_2 value in experiments in the system silicate melt + Fe + C + H_2 at 4 GPa and 1550–1600°C (see text) is also shown.

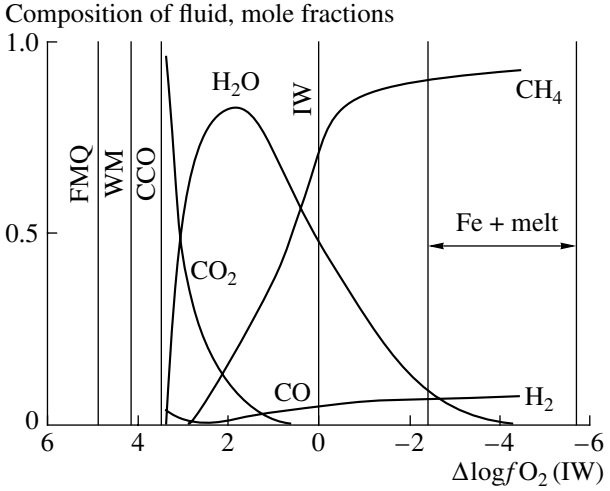

Fig. 3. Composition of C–O–H fluids in equilibrium with graphite as a function of fO_2 in the system at 4 GPa and 1500°C. The C–O–H equilibria were calculated using the data from [35]. Abbreviations of oxygen buffers are the same as in Fig. 2.

The attainment of a very low fO_2 value in the runs was confirmed by the study of redox reactions with the participation of Fe in the melt [12]

$$\text{FeO (melt)} = \text{Fe (metal)} + 1/2\text{O}_2. \quad (1)$$

The addition of 5 and 10 wt % SiC to the starting silicate + graphite mixture allowed us to achieve much lower fO_2 values. The initial SiC was unstable under experimental conditions and was completely consumed according to the reactions

$$\text{SiC (initial)} + \text{O}_2 \longrightarrow \text{SiO}_2\text{ (melt)} + \text{C (graphite)}, \quad (2)$$

and

$$\text{SiC (initial)} \longrightarrow \text{SiC(melt)}. \quad (3)$$

The equilibrium

$$\text{SiC (melt)} + \text{O}_2 = \text{SiO}_2\text{ (melt)} + \text{C (graphite)} \quad (4)$$

controlled fO_2 value during the run along with equilibrium (1).

ESTIMATION OF REDOX STATE OF THE GLASSES PRODUCED DURING MELT QUENCHING

The coefficient of metal–silicate melt fractionation is directly related to fO_2. This relationship may be used to estimate fO_2 in runs when the liquid phase is in equilibrium with metal according to the reaction

$$2\text{FeO (melt)} = 2\text{Fe (metallic phase)} + \text{O}_2. \quad (5)$$

The equilibrium constant of this reaction is written as

$$\log K = \log(a_{\text{FeO}}/a_{\text{Fe}}) - 1/2\log f\text{O}_2^{\text{exp}}, \quad (6)$$

where a_{FeO} and a_{Fe} are the activities of FeO and Fe in the Fe-bearing melt and Fe-alloy, respectively, and $f\text{O}_2^{\text{exp}}$ is determined from high-pressure experiments.

The equilibrium constant of the reaction between pure Fe and pure FeO ($a_{\text{Fe}} = 1$ and $a_{\text{FeO}} = 1$), which is determined by IW buffer, appears as

$$\log K = -1/2\log f\text{O}_2(\text{IW}), \quad (7)$$

where $\log f\text{O}_2(\text{IW})$ is an oxygen fugacity of Fe–FeO equilibrium at P–T conditions of experiment.

The experimental fO_2 values may be presented relative to the IW buffer equilibrium as

$$\log f\text{O}_2^{\text{exp}} = \log f\text{O}_2(\text{IW}) - \Delta\log f\text{O}_2(\text{IW}), \quad (8)$$

where $\Delta\log(\mathrm{IW}) = \log fO_2(\mathrm{IW}) - \log fO_2^{\mathrm{exp}}$ is the difference between $\log fO_{2(\mathrm{IW})}$ and $\log fO_2^{\mathrm{exp}}$ in experiment.

Combining Eqs. (3), (4), and (5), we have

$$\log(a_{\mathrm{FeO}}/a_{\mathrm{Fe}}) - 1/2(\log fO_{2(\mathrm{IW})}) - \Delta\log fO_2(\mathrm{IW}) = -1/2\log fO_2(\mathrm{IW}) \quad (9)$$

and thus

$$2\log(a_{\mathrm{FeO}}/a_{\mathrm{Fe}}) = \Delta\log fO_2(\mathrm{IW}). \quad (10)$$

The activities of Fe and FeO in the phases provide an estimation of fO_2 relative to the Fe–FeO equilibrium. The activity coefficients of FeO in melt at 1550–1600°C were calculated from the data reported in [36].

The obtained fO_2 values fit $\Delta\log fO_2(\mathrm{IW})$ of –2.26 (sample Fb231), –3.67 (sample Fb841), and –5.71 (sample Fb770).

EXPERIMENTAL RESULTS

The experiments were carried out at 4 GPa, 1550–1600°C, and $\Delta\log fO_2(\mathrm{IW}) = -3.86$ and -5.71 ± 0.05. The products of the runs were examined under a microscope in the transmitted and reflected lights. They are yellowish and colorless glasses that contain Fe droplets, 30–100 μm in size, with an exsolution texture that arose during the quenching of the metallic liquid (Figs. 4a, 4b). The Fe droplets mainly cluster at the sample bottom. The spherical shape and dendritic microstructure of the Fe phase indicate that it was liquid during the experiment. Discrete hexagonal graphite crystals, 100–300 μm in size, occur in the glass; graphite particles are also identified at contacts of the metallic phase with glass (Fig. 4b). Separate oval areas, 100–200 μm in size, in the glass contain a finely dispersed graphite phase that amounts to 0.5 wt %. As in the preceding experiments [12], the formation of such areas is likely related to graphite crystallization during quenching. Microscopic and spectral examinations did not reveal inclusions of a C–O–H fluid phase in the glass.

The run products have been studied by several methods, including (1) electron microprobe analysis of samples in order to determine the structure and compositions of phases, (2) infrared and Raman spectroscopy to characterize the H- and C-bearing particles in the glass, and (3) ion microprobe analysis to assess the hydrogen (H_2O) content in the glass.

ANALYSIS WITH ELECTRON MICROPROBE

The analysis of the glass and metallic Fe phase was conducted on a Camebax-microbeam and a Cameca SX100 microprobe at the Institute of Geochemistry and Analytical Chemistry (GEOKhI), Russian Academy of Sciences.

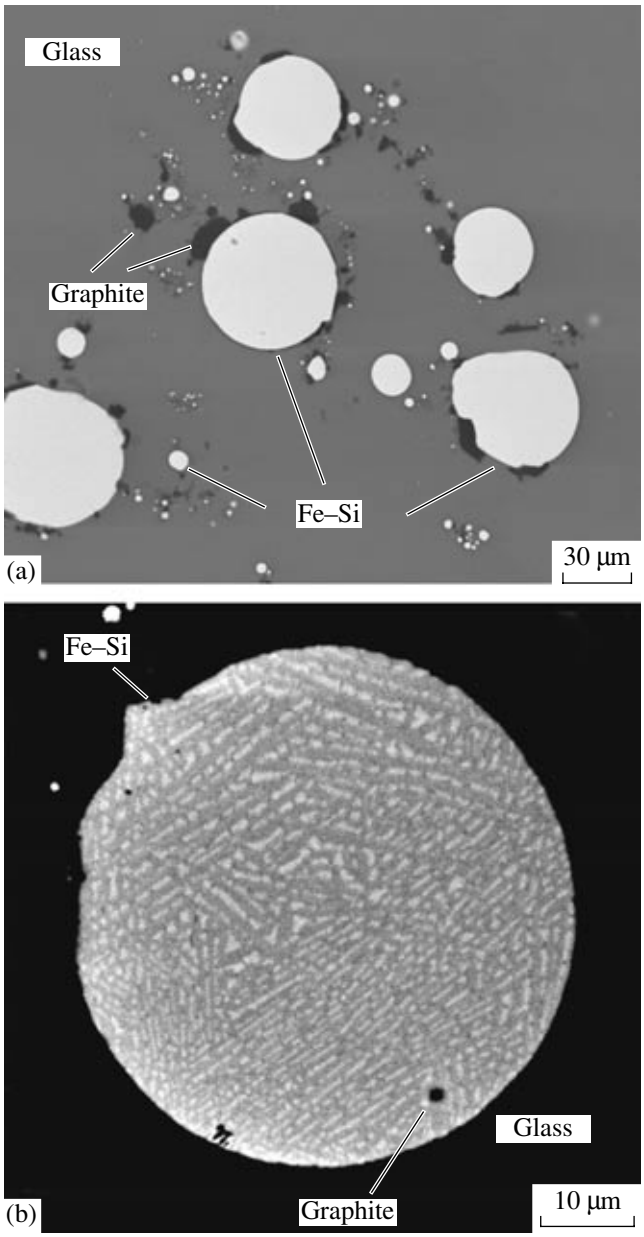

Fig. 4. BSE image of the quenching products. Sample Fb841 after the run at 4 GPa, 1600°C, and $\Delta\log fO_2(\mathrm{IW}) = -3.67$. (a) Glass with droplets of Fe–Si metallic phase and related graphite; (b) microstructure of droplets of Fe–Si metallic phase.

The analytical results are shown in Table 1. The depletion in FeO from 18 wt % in the starting material to 1 wt % in glass is the main chemical feature at $\Delta\log fO_2(\mathrm{IW}) = -5.71$. This feature is a result of FeO reduction with the formation of a liquid Fe phase. The relationship of SiO_2 versus FeO content in glass is shown in Fig. 5. This figure also demonstrates the SiO_2 contents calculated from the assumption that the reduced portion of FeO was removed from silicate liquid. Comparison of these calculations based on equilib-

Table 1. Chemical composition of glass and metallic phase after runs

Run number	Glass														
	P, GPa	*T*, °C	$\Delta\log f O_2$(IW)		SiO_2	TiO_2	Al_2O_3	FeO	MgO	CaO	Na_2O	K_2O	P_2O_5	CoO	NiO	Total
Fb841	4	1600	–3.61	Average of 8	61.61	2.13	13.81	2.90	4.87	9.24	2.79	0.47	0.02	0.02	0.01	97.85
				σ	0.61	0.03	0.20	0.18	0.06	0.14	0.12	0.02	0.02	0.02	0.01	0.61
Fb770	4	1550	–5.71	Average of 8	66.13	1.51	14.42	0.28	5.27	8.82	2.68	0.6	0.16	0.01	0.01	99.89
				σ	0.85	0.08	0.33	0.08	0.08	0.23	0.06	0.01	0.01	0.01	0.01	0.96

Run number	Metallic phase									
	P, GPa	*T*, °C	$\Delta\log f O_2$(IW)		Fe	Si	P	W	Pt	Total
Fb841	4	1600	–3.61	Average of 5	93.06	0.14	1.04	Ì.Ó.	0.26	94.50
				σ	0.81	0.03	0.12	–	0.17	0.88
Fb770	4	1550	–5.71	Average of 5	84.43	8.54	0.93	0.02	0.02	93.94
				σ	0.38	0.93	0.29	0.00	0.00	0.61

rium of Fe with Fe-bearing melt (1) indicates that the crystallization of Fe is responsible for the modified chemical composition of the melt. However, at $\Delta\log f O_2$(IW) = –5.71, the SiO_2 content is higher than it follows from calculations. This may be accounted for by the addition of some amount of SiC to the silicate liquid according to reaction (2).

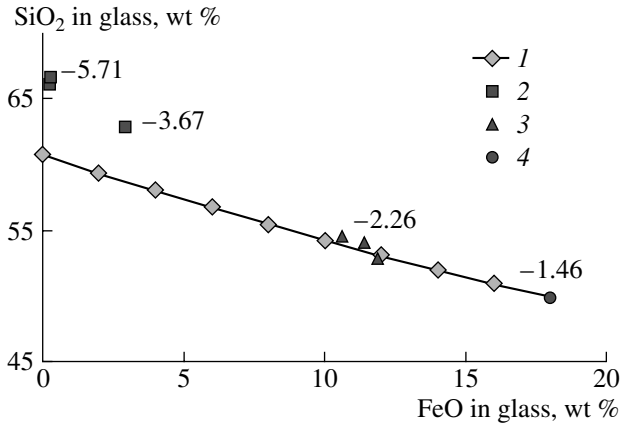

Fig. 5. SiO_2 contents in glasses versus FeO content controlled by $f O_2$ values during experiments at 4 GPa and 1550–1600°C. (*1*) glass composition calculated under the assumption that part of FeO reduced during the experiment was removed from the melt; (*2*) glass composition after runs with sample Fb841, $\Delta\log f O_2$(IW) = –3.67 and sample Fb770, $\Delta\log f O_2$(IW) = –5.71; (*3*) glass composition after runs at 3.7 GPa, 1520–1600°C, and $\Delta\log f O_2$(IW) = –2.31 ± 0.05 [12]; (*4*) initial FeO content in the silicate fraction of the starting mixture, $\Delta\log f O_2$(IW) = –1.46. The SiO_2 contents in samples Fb841 and Fb770 are above the calculated values owing to the dissolution of initial SiC in the melt according to reactions (1)–(3).

The Fe contents in the tungsten foil and platinum capsule are below 0.1 wt %; the Pt contents in the tungsten and W in the platinum are also below 0.1–1.0 wt %. Thus, the effect of the Pt walls of the capsule and the W foil on the extraction of Fe from the Fe-bearing melt was very small.

Globules of metallic Fe phase were analyzed and compared with the known C-bearing Fe alloys. The results obtained yielded 5–6 wt % C.

SPECTROSCOPY OF H- AND C-BEARING GLASSES—PRODUCTS OF MELT QUENCHING

The infrared and Raman spectra of the glasses produced by melt quenching after the high-pressure experiments served as the basis for the determination of hydrogen and oxygen bonds in melts and, hence, the mechanisms of H and C dissolution in silicate melt as a function of $f O_2$. The compared $f O_2$ values in runs at 4 GPa and 1550–1600°C correspond to $\Delta\log f O_2$(IW) of –2.26 (sample Fb231), –3.67 (sample Fb841), and –5.71 (sample Fb770). The spectral characteristics of glasses at $\Delta\log f O_2$(IW) = –2.26 were reported in [12].

INFRARED SPECTROSCOPY OF GLASSES

In order to measure the transmission spectra of the quenched glasses, thin doubly polished plates were prepared. The thickness of the glass was determined using the micrometric facilities of an optical microscope with

an accuracy of ±3 μm. The IR measurements were carried out with an IFS-113v (Bruker) Fourier spectrometer combined with an optic microscope. The typical FTIR spectra of C–H-bearing glasses of samples Fb231, Fb841, and Fb770 are shown in Figs. 6 and 7.

O–H *bonds.* A wide asymmetric absorption band at frequencies of 3490–3520 cm^{-1} is a notable feature of the high-frequency region of the glass spectrum (above 3000 cm^{-1}) for $\Delta\log fO_2(IW) = -2.26$ and –3.67 (Figs. 6a, 6b). This band is a result of valence oscillations of the OH^- group and molecules of H_2O [37, 38]. The weak absorption line at 4510 cm^{-1} for $\Delta\log fO_2(IW) = -2.26$ and at 4446 cm^{-1} for $\Delta\log fO_2(IW) = -3.67$ belongs to the composite oscillation of OH groups and the glass network. The peak at 1626–1632 cm^{-1} (Fig. 7a) fits the deformational oscillation of H_2O molecules [39]. At passing to very low fO_2 values ($\Delta\log fO_2(IW) = -5.71$), the absorption bands at 3540 and 1630 cm^{-1} become much less intense (Fig. 6c).

H–H *bonds.* The spectra reveal a very weak absorption band near 4117–4123 cm^{-1} (Fig. 6a). This band is thought to pertain to molecular hydrogen dissolved in the glass [39].

C–O *bonds.* The wide weak band with a maximum within a region of 2360–2370 cm^{-1} for $\Delta\log fO_2(IW) = -2.26$ (Fig. 6a) is interpreted as a result of oscillations of the CO_2 molecule. According to [40], carbonates dissolved in silicate glasses have characteristic absorption bands at 1600–1380 cm^{-1}. At $\Delta\log fO_2(IW) = -2.26$, wide and weak peaks on 1430–1435 cm^{-1} (Fig. 6a) are noticed. At $\Delta\log fO_2(IW) = -3.67$ and –5.71, no peaks at 1430–1435 cm^{-1} were identified. At the same time, a wide and weak band within a region of 2360–2370 cm^{-1} is retained at $\Delta\log fO_2(IW) = -3.67$ (Fig. 6b).

C–H *bonds.* The appearance of absorption bands within the region of 2900–3100 cm^{-1} (3072–3076, 2957–2959, and 2989 cm^{-1}) is characteristic of the spectra at $\Delta\log fO_2(IW) = -3.67$ and –5.71 (Figs. 6b and 6c). According to [41], they correspond to the oscillations of molecular CH_4 or other hydrocarbon groups, for example, CH_3 or CH_2. This indicates that the bonds of the C–H type are present in the bands under reducing conditions and at $\Delta\log fO_2(IW) = -3.67$ and –5.71. It is possible that some absorption bands in the region of 1300–1400 cm^{-1} (Figs. 7b and 7c) also fit the oscillations of hydrocarbon groups (1399 and 1368 cm^{-1}).

Double peak on 1720 and 1744 cm^{-1}. At $\Delta\log fO_2(IW) = -3.67$ and –5.71, an acute intense peak at 1722 cm^{-1} is revealed in the first case and a double peak at 1720 cm^{-1} and 1744 cm^{-1} is seen in the second case. According to [42], an intense double peak within the region of 1740–1710 cm^{-1} is typical of the C=O bond. It is suggested that such a bond is formed in glass at a low $\Delta\log fO_2(IW)$ (Figs. 7b and 7c).

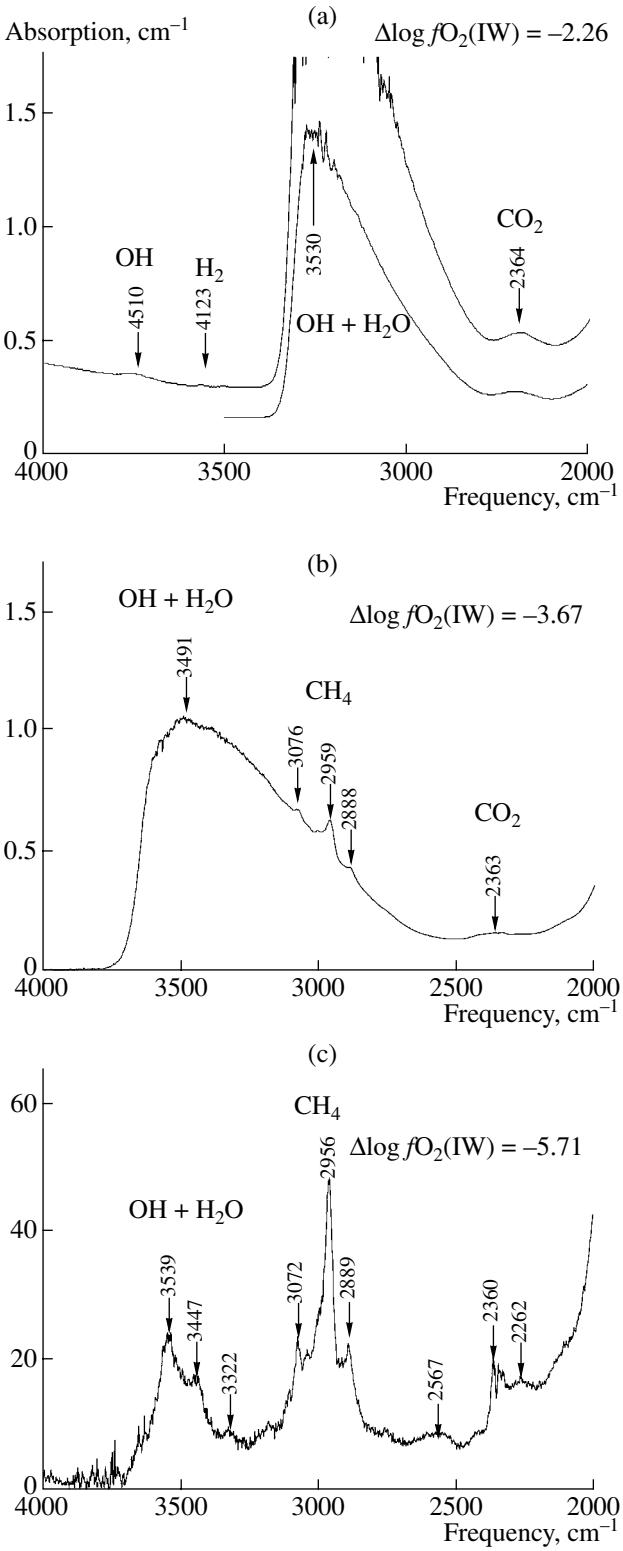

Fig. 6. IR spectra of C- and H-bearing glasses in a region of 5000–2000 cm^{-1} at various fO_2 during experiments at 3.7–4.0 GPa and 1550–1600°C for the following samples: (a) Fb231, thickness is 121 ± 2 and 240 ± 3 μm, $\Delta\log fO_2(IW) = -2.26$; (b) Fb841, thickness is 121 ± 2 μm and $\Delta\log fO_2(IW) = -3.67$; (c) Fb770, thickness is 110 ± 2 μm and $\Delta\log fO_2(IW) = -5.71$. Data for sample Fb231 are taken from [12].

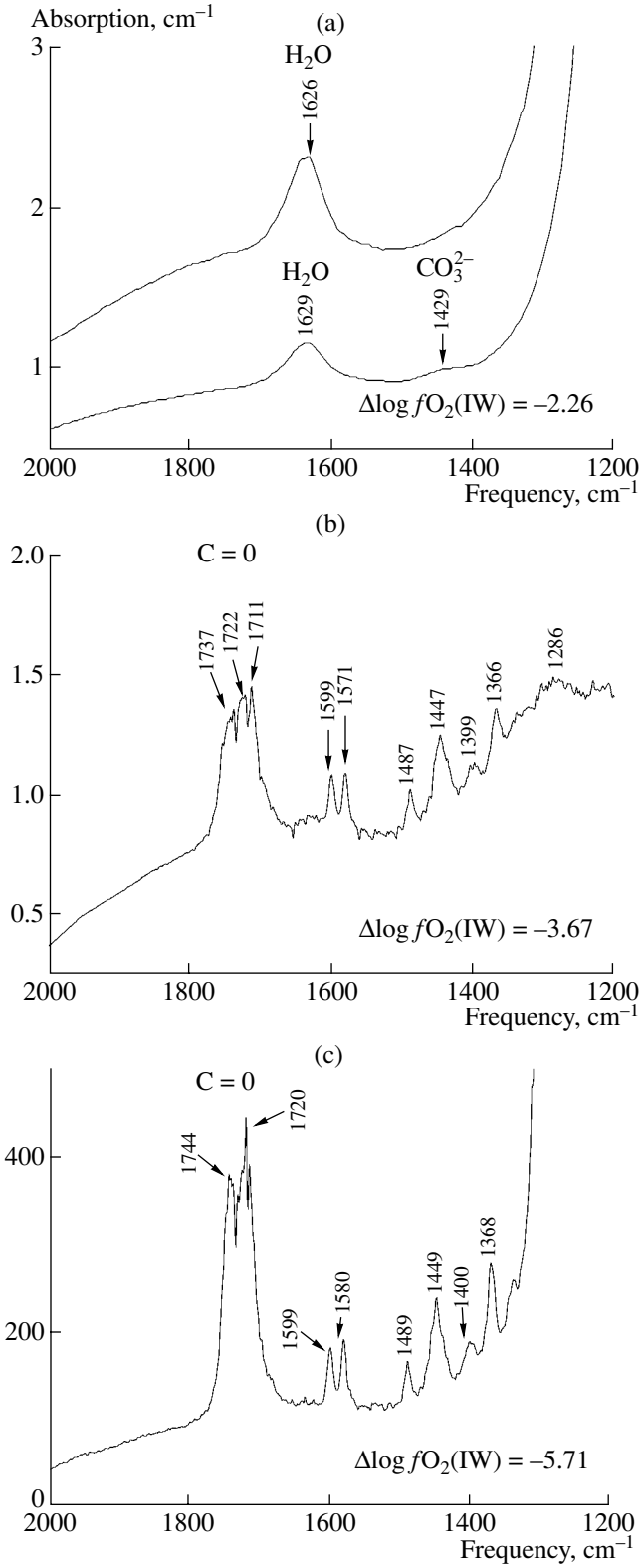

Fig. 7. IR spectra of C- and H-bearing glasses in the region of 2000–1000 cm^{-1}. See Fig. 6 for explanation.

Peaks at 1580 and 1599 cm^{-1}. The nature of these acute peaks in glass (Figs. 7b and 7c) is ambiguous. In the Raman spectra, they mark C–C bonds in glass or the graphite phase.

RAMAN SPECTROSCOPY OF GLASSES

The Raman spectroscopy of H- and C-bearing glasses for ΔlogfO_2(IW) of –2.26 (sample Fb231), –3.67 (sample Fb841), and –5.71 (sample Fb770) was conducted on a T64000 Raman spectrograph (Jobin Yvon). The characteristic Raman spectrum of samples within the region of 400–4300 cm^{-1} are shown in Figs. 8–10.

O–H *bonds.* The Raman spectra within the high-frequency region (3000–3800 cm^{-1}) contain a wide and asymmetric band at 3560–3590 cm^{-1} (Fig. 8a). The shape of this band is similar to that found in water-bearing glasses [43] and water-bearing glasses in the Na_2O–Al_2O_3–SiO_2 system [44]. This band fits oscillations of O–H bonds in the molecule of H_2O or in OH^- groups in the structure of silicate melts. A decrease in the intensity of this band with decreasing fO_2 was detected.

H–H *bonds.* A band on 4136 cm^{-1} at ΔlogfO_2(IW) = –3.67 (Fig. 8b) belongs to molecular hydrogen dissolved in the glass [44].

C–H *bonds.* The Raman spectroscopy within the region of oscillations pertaining to C–H bonds reveal peaks on 2920–2930, 3070, and 2724 cm^{-1}. They are poorly expressed at ΔlogfO_2(IW) = –2.26 and are distinct at ΔlogfO_2(IW) = –3.67 (Figs. 9a and 9b).

Si–C *bonds.* The Raman spectra of glasses within a region of 200–1200 cm^{-1} and at ΔlogfO_2(IW) = –2.26, –3.67, and –5.71 are shown in Figs. 10a and 10b. The Raman spectra were also measured for comparative purposes in the glass obtained by quenching melts from the runs at 1 atm and 1300°C and at ΔlogfO_2(IW) = –2.26 (Fig. 8a). As in the experiments under a high pressure, the ferrobasaltic melt was reduced with the formation of an Fe phase. Three bands: 912, 852, and 494 cm^{-1} were revealed in this sample. They fit the frequency bands established in all aluminosilicates in the regions of 900–1200, 800–850, and 500–600 cm^{-1} [45, 46]. Similar bands were also detected in the glasses after the high-pressure runs, however, the two former bands display a lower frequency, probably owing to the dissolution of C and H in the melts (Figs. 10a and 10b).

A band at 784–792 cm^{-1} (Figs. 10a and 10b), which is absent from the starting glass, is observed in all samples after runs at a high pressure. This oscillatory peak may be ascribed to the Si–C bond typical of moissanite [47]. The Raman spectrum of a synthetic SiC crystal demonstrates two acute bonds at 785.7 and 767 cm^{-1} (Fig. 10c).

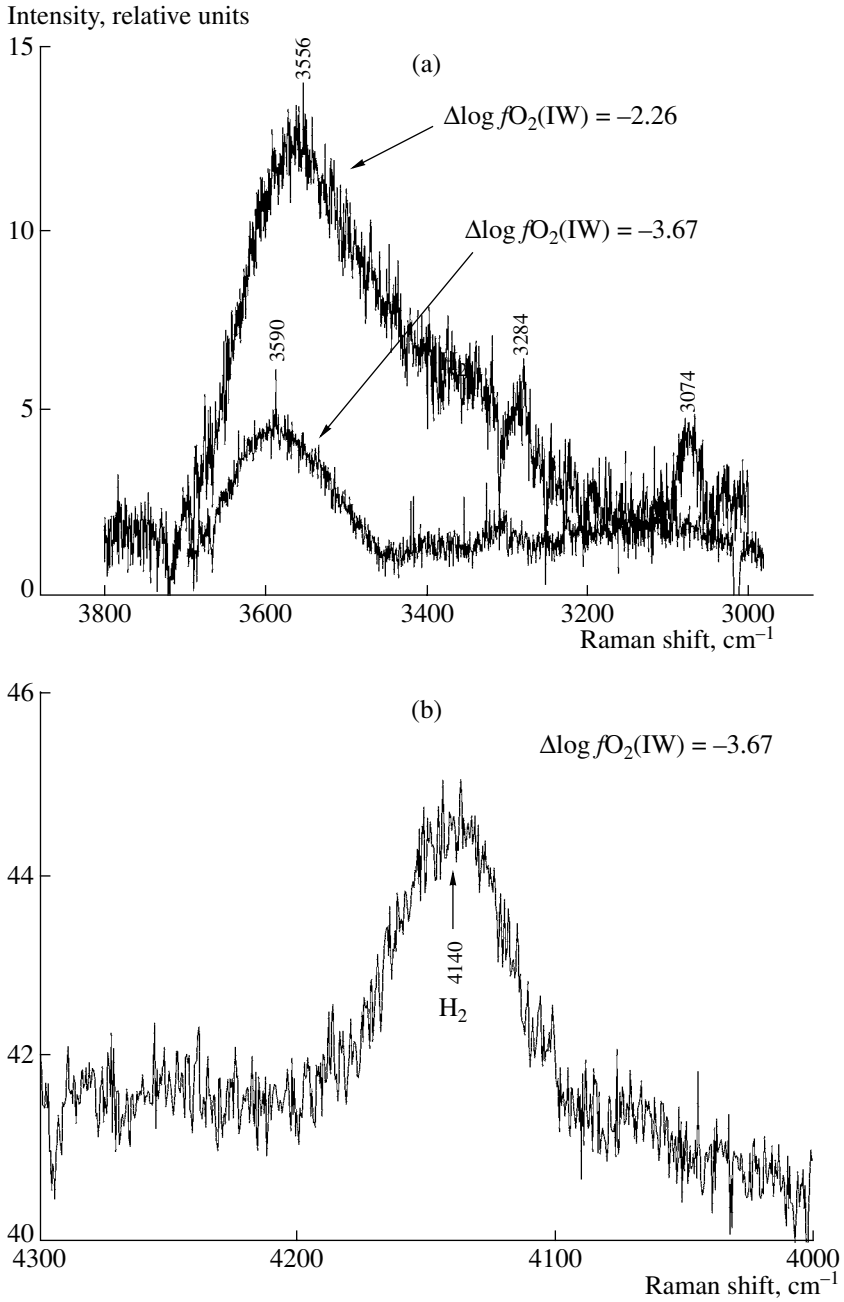

Fig. 8. Raman spectra of C- and H-bearing glasses in a region of oscillations of O–H and H–H bonds. (a) Fb231, $\Delta\log f\,O_2(IW) = -2.26$ and Fb841, $\Delta\log f\,O_2(IW) = -3.67$; (b) Fb841, $\Delta\log f\,O_2(IW) = -3.67$. Data for sample Fb231 are taken from [12].

Graphite. The focusing of the laser beam on the glass regions with small black inclusions reveals a peak at 1598 cm^{-1} at $\Delta\log f\,O_2(IW) = -2.26$, an acute intense peak at 1577 cm^{-1} and a wide intense band at $\Delta\log f\,O_2(IW) = -5.71$ (Fig. 11a). These oscillations correspond to graphite [48]. The graphite disc located in the upper portion of sample during the experiments yields an acute peak at 1582 cm^{-1} and a band at 1359 cm^{-1} (Fig. 11b). Following Lespade *et al.* [48] and Rouzaud *et al.* [49], we related bands at 1578–1598 and 1347–1365 cm^{-1} to the region of C–C oscillations in graphite with various degrees of lattice ordering. According to the authors cited above, the band at 1580 cm^{-1} becomes wider with a decrease in the degree of crystallinity and is shifted to the higher frequency region with the simultaneous appearance of a wide band at ~1350 cm^{-1}. In our experiment, the band at ~1350 cm^{-1} becomes wider and more intense, shifting toward lower frequencies.

The band at a frequency of 1052 cm^{-1} corresponds to silicate glass, which occurs in aggregates with graph-

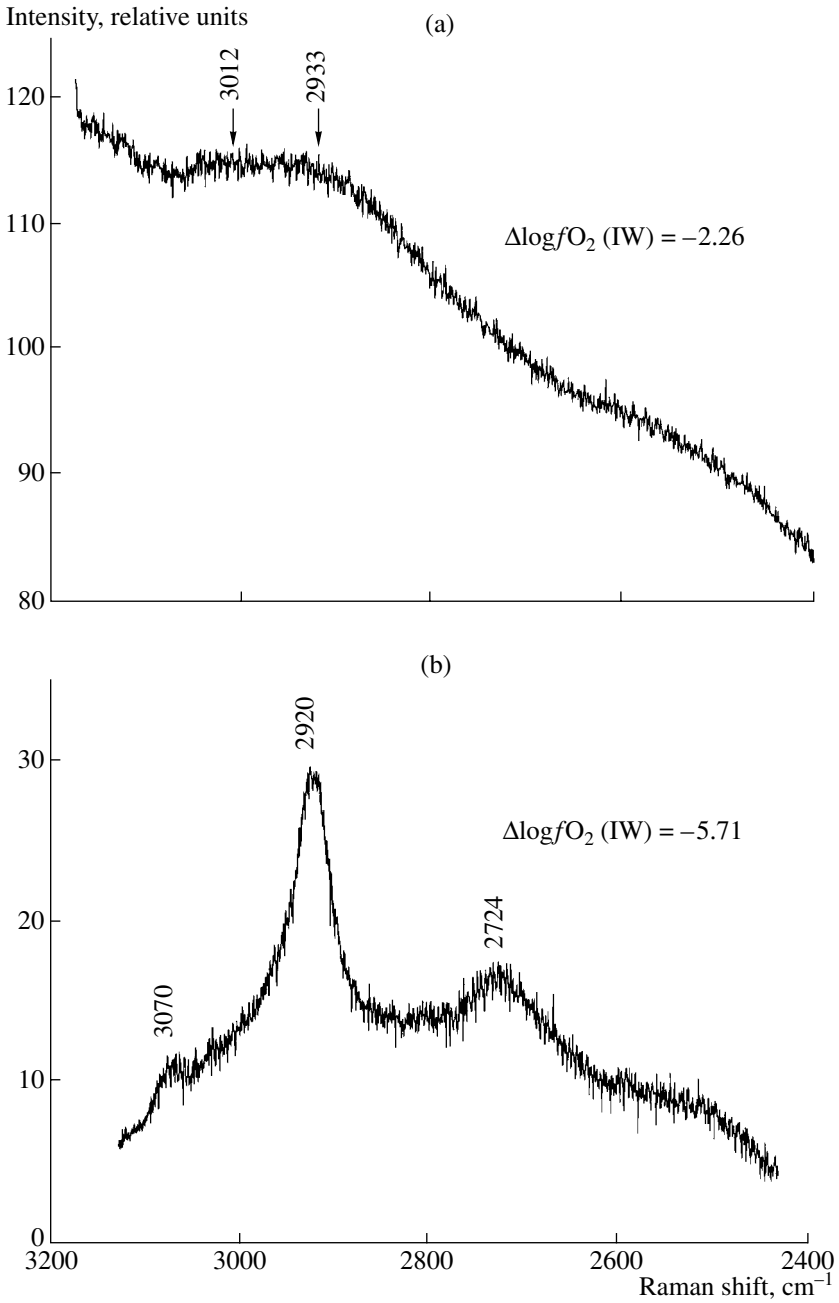

Fig. 9. Raman spectra of C- and H-bearing glasses in a region of oscillations of C–H bonds. (a) Fb231, $\Delta\log fO_2$(IW) = –2.26; (b) Fb770, $\Delta\log fO_2$(IW) = –5.71.

ite crystals, and the weak lines at 794 and 797 cm^{-1} were attributed to bonds like Si–C in graphite or in glass in aggregates with graphite, as was discussed above (Fig. 10b).

EFFECT OF fO_2 UPON THE FORMATION OF C–H BONDS IN MELT

The infrared and Raman spectroscopy of glasses indicates a remarkable feature of C–H interaction with a reduced silicate: an appreciable change in the mechanism of their dissolution with a decrease in fO_2. The melting at $\Delta\log fO_2$(IW) = –2.26 produces a melt with the hydroxyl group as the prevalent hydrogen species in the melt, whereas melting at $\Delta\log fO_2$(IW) = –5.71 results in the accommodation of hydrogen in the melt mainly due to C–H bonds (as CH_4). This circumstance provides insights into the conditions of magmatic transport of hydrogen compounds and carbon from the deep zones of reduced planetary matter.

DETERMINATION OF $^1H^+/^{30}Si^+$ IN H- AND C-BEARING GLASSES WITH ION MICROPROBE

Thin polished sections were prepared to measure the $^1H^+/^{30}Si^+$ ratios in glasses with a Cameca IVS 3f ion microprobe at the Institute of Microelectronics and Information, Russian Academy of Sciences, in Yaroslavl. The samples were subjected to ultrasonic cleaning and were coated with gold. The intensity of $^1H^+$ and $^{30}Si^+$ peaks was measured under bombardment with a O_2^- beam (at a current of 10–15 nA, a beam size of 10 μm, mass resolution of 1200, and filtration energy of 100 ± 20 V). The H_2O (H) contents in glasses were assessed using a calibration curve [50]. This curve was calibrated on the ratio of H_2O content (wt %) to SiO_2 (wt %) within the interval of H_2O contents from 0.09 to 8.0 wt %. No substantial effect of the standard matrix upon measurement results has been detected in a range of silica contents from 49 to 71 wt %.

It should be noted that the experiments in the system silicate melt (ferrobasalt) + liquid Fe phase (with 2–8 wt % of Si) + graphite + SiC + H_2 correspond to the region of low fO_2 values, so that hydrogen occurs in glasses not only as OH^- group but also as H_2. Therefore, the H_2O content in glasses estimated with the above calibration curve [50] should be regarded as the maximum estimate. The measurements indicate that the water content in the glasses reaches 0.87–1.65 wt % (Table 2) and decreases with decreasing fO_2 in consistence with the results of IR spectroscopy.

MAGMATIC TRANSFER OF HYDROGEN COMPOUNDS AND CARBON FROM THE DEEP-SEATED ZONES OF REDUCED PLANETARY MATTER

The solubility of volatile compounds in magmas and the redox state of their mantle source are the main factors that control the transfer of volatile components from the planet's interior to its surface. In theories of the formation of the Earth, the composition of gases extracted by primary planetary magmas is accounted for by the large-scale melting of the early mantle that occurred in the presence of the metallic Fe phase [1, 2]. The Fe alloy and the fused silicate material underwent gravitational migration that exerted influence on the formation of the metallic core of the planet. The large-scale melting of the early Earth should have been accompanied by the formation of volatile compounds whose composition was controlled by the interaction of H and C with silicate and metallic melts; many aspects of this process remain badly understood as of yet.

The experimental study reported in this paper, together with previous investigations [12], allow us to propose some explanations of the formation of hydrogen and carbon compounds in silicate liquids in the presence of a metallic Fe phase.

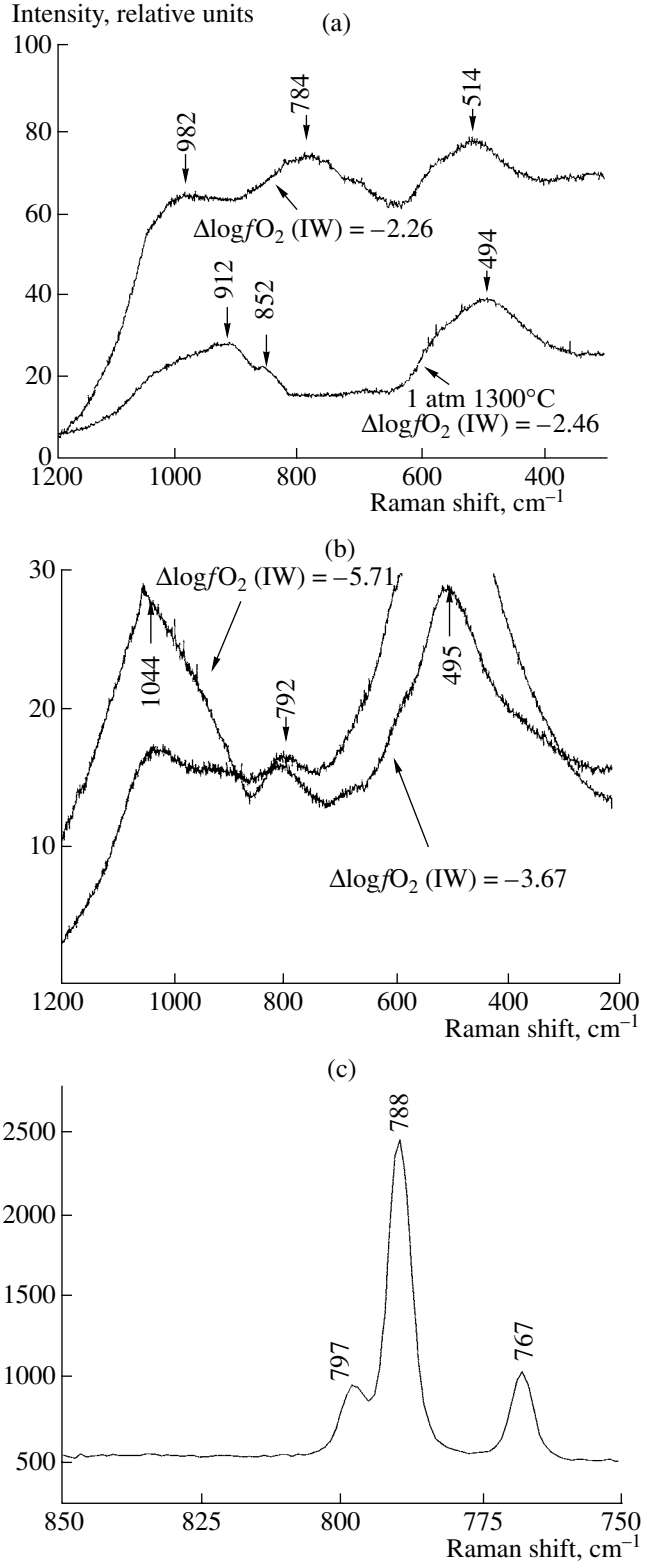

Fig. 10. Raman spectra of C- and H-bearing glasses in a region of oscillations of Si–C bonds. (a) Fb231, ΔlogfO_2(IW) = –2.26 and ΔlogfO_2(IW) = –2.46 after run at 1 atm and 1300°C; (b) Fb841, ΔlogfO_2(IW) = –3.67 and Fb770, ΔlogfO_2(IW) = –5.71; (c) crystal SiC [12].

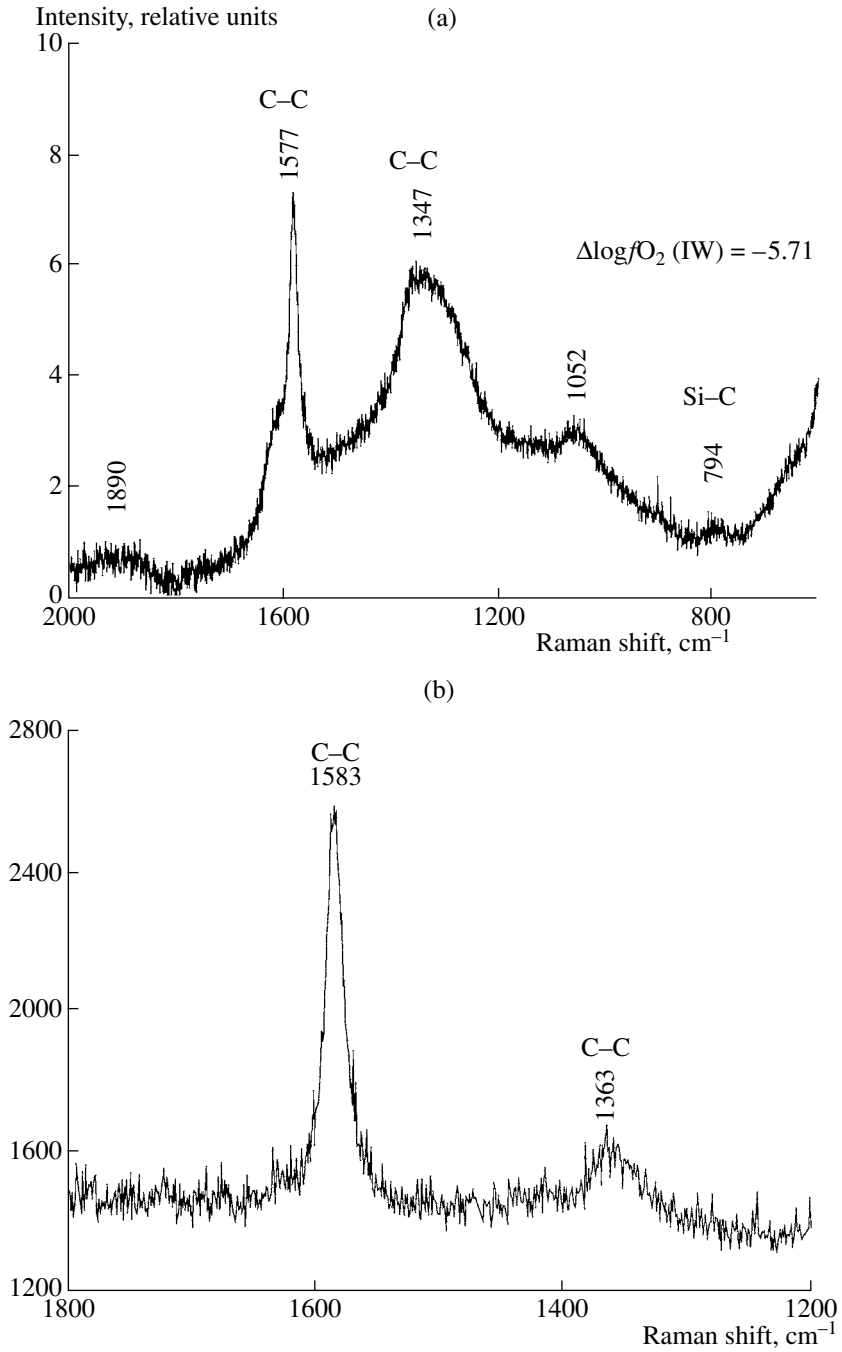

Fig. 11. Raman spectra of graphite crystals from samples of C- and H-bearing glasses. (a) Fb770, ΔlogfO_2(IW) = –5.71; (b) graphite disc (Fig. 1, Fb231, ΔlogfO_2(IW) = –2.26).

The nature of H and C compounds dissolved in silicate melts was characterized in a series of runs in the system Fe-bearing melt + fused metallic Fe phase (0.1–0.7% Si) + C (graphite) + H_2 at 4 GPa and 1550–1600°C. This study in the stability field of the Fe–Si metallic phase under a pressure corresponding to a depth of 100–150 km has shown that melting gives rise to the formation of silicate liquids containing H and C in both oxidized and reduced modes, in proportions depending on fO_2.

According to [12], hydrogen occurs in the melt largely as the OH^- group and H_2O at ΔlogfO_2(IW) = –(2.0–2.5). Some amount of hydrogen is dissolved in the molecular form. Carbon is soluble in the melt mainly in the atomic form and as insignificant quantities of the carbonate ion CO_3^{2-}; carbon is also bound in the melt with Si (Si–C-type bond). Thereby, the melts are characterized by the preferential dissolution of H in comparison with C.

The character of H and C dissolution substantially changes at a lower $\Delta\log fO_2(IW) = -(4–6)$ in the presence of a Fe–Si liquid phase. The solubility of H in the form of OH^- decreases, while the solubility of H as H_2 increases. The solubility of carbon is related to the formation of the C–H bond in the melt; this bond corresponds to CH_4. The amount of dissolved H recalculated to water decreases with falling fO_2 from 1.6–1.8 wt % H_2O at $\Delta\log fO_2(IW) = -2.3$ to 0.8–1.0 wt % H_2O at $\Delta\log fO_2(IW) = -5.71$. At the same time, the carbon solubility increases from 0.2 wt % at $\Delta\log fO_2(IW) = -2.3$ to approximately 2 wt % at $\Delta\log fO_2(IW) = -5.71$.

The experimental studies lead to the conclusion that the proportions of reduced and oxidized carbon species in the primary magma substantially depend on fO_2 in the reduced mantle. At $\Delta\log fO_2(IW) \approx -2$, which corresponds to the equilibrium of Fe with olivine occurring in the upper mantle, oxidized H species are predominant in the melt equilibrated with metallic Fe. If the chemical fractionation of the early mantle proceeded at a lower fO_2, e.g., at $\Delta\log fO_2(IW) = -(3–5)$, then the formation of compounds with C–H-type bond (CH_4 and other molecules with this bond) should be expected in the primary magmas, along with oxidized H species (OH^- group). These volatile compounds of H and C are associated with the formation of a liquid Fe phase enriched in Si.

Thus, the regime of fO_2 during the formation of the magmatic ocean is of principal importance for the estimation of the composition of gases that could have been extracted from the reduced planetary matter and come to the surface in the course of high-temperature volcanic activity.

The transition of crystalline silicate matter into the fused state must be crucial in determining the primary composition of the volatile components of the Earth. One of the main features of redox reactions in melts is determined by the fact that, despite the oxygen fugacity is below the IW buffer, oxidized hydrogen and carbon species (H_2O, OH^-, CO_3^{2-}) remain stable [12, 27, 51]. This specific feature of H_2 and C interaction with silicate melts may be critical for the transformation of reduced H and C species that were contained in the early mantle [3, 21] into species that are predominant in the modern mantle (OH^-, H_2O, and CO_3^{2-}). Conceivably, the chemical evolution of hydrogen and carbon during early episodes in the evolution of reduced mantle should have been strongly affected by liquid metallic Fe formed by magma reduction. The regime of fO_2 during the formation of the magmatic ocean is of principal importance for the estimation of the composition of gases with respect to H_2O, H_2, and CH_4 that could have been extracted from the reduced planetary matter and supplied to the surface in the course of high-temperature volcanic activity. The enstatite-chondrite model of the Earth formation [3] requires the enrichment of the gases in CH_4 and H_2.

Table 2. H_2O content in H- and C-bearing glasses

Run	$\Delta\log fO_2(IW)$	H_2O, wt %
Fb231	–2.26	1.65 ± 0.03
Fb841 5K	–3.69	1.16 ± 0.012
Fb770 3K	–5.71	0.87 ± 0.03

CONCLUSIONS

(1) A series of experiments in the system Fe-bearing melt + fused metallic Fe phase (0.1–7% Si) + C (graphite) + H_2 at 4 GPa, 1550–1600°C, and $\Delta\log fO_2(IW) = -3.67$ and –5.71 characterizes the nature of H and C compounds dissolved in silicate melts. The infrared and Raman spectroscopic measurements of the glasses produced by reduced melt quenching were used in order to elucidate the mechanisms of H and C dissolution.

(2) The study of the stability field of the metallic Fe–Si phase at pressures corresponding to depths of 100–150 km has shown that melting results in the formation of silicate liquids containing H and C both in the oxidized and reduced forms. Their proportions strongly depend on fO_2.

(3) At $\Delta\log fO_2(IW) = -2.4$, hydrogen occurs in the melt largely as the OH^- group and H_2O [12]. Some amount of hydrogen is dissolved in the molecular form. Carbon is dissolved mainly in the atomic form and insignificantly as the carbonate ion CO_3^{2-}. Experiments at lower $\Delta\log fO_2(IW)$ values of –3.67 and –5.71 in the presence of a liquid Fe–Si phase showed a marked change in the character of H and C dissolution in the reduced melt. The solubility of hydrogen as OH^- decreases, while its solubility as H_2 increases. The solubility of carbon increases owing to the formation of the C–H bond corresponding to CH_4 in the melt.

(4) The experimental investigations lead to the conclusion that the proportions of reduced and oxidized carbon species in the primary melts appreciably depend on the fO_2 values in the reduced mantle. At $\Delta\log fO_2(IW) \approx -2$, which corresponds to equilibrium between Fe and olivine in the upper mantle, oxidized hydrogen species are predominant in the melt equilibrated with metallic Fe. If the chemical differentiation of the early mantle proceeded at lower fO_2 values at $\Delta\log fO_2(IW) = -(3–5)$, then the compounds with the C–H-type bond (CH_4 and other molecules with this bond) could be expected in the primary melts along with oxidized hydrogen species (group OH^-).

ACKNOWLEDGMENTS

The authors thank Acad. E.M. Galimov for the fruitful discussion of the manuscript.

This work was carried out under the Program of Fundamental Research of the Division of Earth Sciences, Russian Academy of Sciences "Deep Structure of the Earth, Geodynamics, Magmatism, and Interaction of Geospheres," project "Evolution of the Redox State and Gas Regime of the Earth and Its Effect on the Interaction of Geospheres" and under the State contract with the Institute of Experimental Mineralogy, Russian Academy of Sciences, project "Formation of Volatiles by Melting of the Reduced Mantle" under the Program of Fundamental Research no. 9 of the Division of Earth Sciences, Russian Academy of Sciences "Experimental Studies of Physicochemical Problems of Geological Processes and the Russian Foundation for Basic Research, project no. 05-05-64391."

REFERENCES

1. G. W. Wetherill, "Formation of the Earth," Annu. Rev. Earth Planet. Sci. **18**, 205–256 (1990).
2. M. J. Walter, H. E. Newsom, W. Ertel, and A. Holzheid, "Silicate Partitioning and Implications for Core Formation," in *Origin of the Earth and Moon*, Ed. by R. M. Canup and K. Righter (Univ. Arizona Press, Tucson, 2000), pp. 265–289.
3. M. Javoy, "The Integral Enstatite Chondrite Model of the Earth," Geophys. Rev. Lett. **22**, 2219–2222 (1995).
4. Y. Abe, E. Ohtani, T. Okuchi, *et al.*, "Water in the Early Earth," in *Origin of the Earth and Moon*, Ed. by R. M. Canup and K. Righter (Univ. Arizona Press, Tucson, 2000), pp. 413–433.
5. T. C. Owen and A. Bar-Nun, "Volatile Contributions from Icy Planetesimals," in *Origin of the Earth and Moon*, Ed. by R. M. Canup and K. Righter (Univ. Arizona Press, Tucson, 2000), pp. 459–471.
6. C. Hayashi, K. Nakazawa, and Y. Nacagawa, "Formation of the Solar System," in *Protostars and Planets II*, Ed. by D. C. Black and M. S. Matthons (Univ. Arizona Press, Tucson, 1985), pp. 1100–1153.
7. H. Wanke and G. Dreibus, "Chemistry and Accretion of Earth and Mars," LPC **XV**, 884–885 (1984).
8. D. Porcelli and R. O. Pepin, "Rare Gas Constraints on Early Earth History," in *Origin of the Earth and Moon*, Ed. by R. M. Canup and K. Righter (Univ. Arizona Press, Tucson, 2000), pp. 435–458.
9. Y. Abe, "Physical State of Very Early Earth," Lithos **30**, 223–235 (1993).
10. S. Sasaki, "The Primary Solar-Type Atmosphere Surrounding the Accreting Earth: H_2O-Induced High Surface Temperature," *in Origin of the Earth*, Ed. by H. E. Newsom and J. H. Jones (Oxford Univ., New York, 1990), pp. 195–209.
11. E. M. Galimov, *Life Phenomenon: between Equilibrium and Non-Linearity. Origin and Principles of Evolution* (URSS, Moscow, 2001) [in Russian].
12. A. A. Kadik, F. Pineau, Y. A. Litvin, *et al.*, "Formation of Carbon and Hydrogen Species in Magmas at Low Oxygen Fugacity during Fluid-Absent Melting of Carbon-bearing Mantle," J. Petrol. **45** (7), 1297–1310 (2004).
13. I. D. Ryabchikov, D. Green, V. Wall, and D. Brey, "Oxidation State of Carbon in the Low-Velocity Zone," Geokhimiya, No. 2, 221–232 (1981).
14. R. J. Arculus, "Oxidation Status of the Mantle: Past and Present," Annu. Rev. Earth Planet. Sci. **13**, 75–95 (1985).
15. W. R. Taylor, and D. H. Green, "The Petrogenetic Role of Methane: Effect on Liquidus Phase Relations and the Solubility Mechanism of Reduced C–H Volatiles," in *Magmatic Processes: Physicochemical Principles*, Ed. by B. O. Mysen, Geochem. Soc. Spec. Publ. **1**, 121–138 (1987).
16. C. Ballhaus, "Redox States of Lithospheric and Asthenospheric Upper Mantle," Contrib. Mineral. Petrol. **114**, 331–348 (1993).
17. J. F. Kasting, D. H. Eggler, and S. P. Raenburn, "Mantle Redox Evolution and Oxidation State of the Archean Atmosphere," J. Geol. **101**, 245–257 (1993).
18. A. A. Kadik, "Evolution of Earth's Redox State during Upwelling of Carbon-Bearing Mantle," Phys. Earth Planet. Int. **100**, 157–166 (1997).
19. E. M. Galimov, "Growth of the Earth's Core as a Source of Its Internal Energy and a Factor of Mantle Redox Evolution," Geokhimiya, No. 8, 755–758 (1998) [Geochem. Int. **36** (8), 673–675 (1998)].
20. L. N. Kogarko, "Alkaline Magmatism in the Early History of the Earth," Petrologiya **6** (3), 251–258 (1998) [Petrology **6** (3), 230–236 (1998)].
21. M. Javoy, "The Major Volatile Elements of the Earth: Origin, Behavior, and Fate," Geophys. Rev. Lett. **24**, 177–180 (1997).
22. M. Javoy, "The Birth of the Earth's Atmosphere: The Behavior and Fate of the Major Elements," Chem. Geol. **147**, 11–25 (1998).
23. B. J. Wood, L. T. Bryndzia, and K. E. Johnson, "Mantle Oxidation State and Its Relationship to Tectonic Environment and Fluid Speciation," Science **248**, 337–345 (1990).
24. H. Wanke, "Constitution of Terrestrial Planets," Phil. Trans. R. Soc. London **A303**, 287–302 (1981).
25. C. J. Allegre, J.-P. Poirier, E. Hulmer, and A. W. Hofman, "The Chemical Composition of the Earth," Earth Planet. Sci. Lett. **134**, 515–526 (1995).
26. D. H. Eggler and D. Baker, "Reduced Volatiles in the System C–O–H: Implications to Mantle Melting, Fluid Formation, and Diamond Genesis," in: *High Pressure Research in Geophysics*, Ed. by S. Akimoto and M. Manghnani (Jpn. Cent. Acad. Public., Tokyo, 1982), pp. 237–250.
27. J. R. Holloway and S. Jakobsson, "Volatile Solubilities in Magmas: Transport of Volatiles from Mantles to Planet Surface," J. Geophys. Res. **91** (B4), D505–D508 (1986).
28. N. I. Bezmen, V. A. Zharikov, M. B. Epelbaum, *et al.*, "The System $NaAlSi_3O_8$–H_2O–H_2 (1200°C, 2 kbar): The Solubility and Interaction Mechanism of Fluid Species with Melt," Contrib. Mineral. Petrol. **109**, 89–97 (1991).

29. A. Kadik, F. Pineau, Y. Litvin, *et al.*, "Formation of Carbon and Hydrogen Species in Magmas at Low Oxygen Fugacity," UK J. Conf. Abstracts **5** (2), 564 (2000).
30. Yu. A. Litvin, "On the Procedure for the High-Pressure Studies of Phase Equilibria with Iron-bearing Magmatic Melts," Geokhimiya, No. 8, 1234–1242 (1981).
31. S. R. Bohlen and A. L. Boettcher, "The Quartz–Coesite Transformation: A Precise Determination and the Effects of Other Components," J. Geophys. Res. **87**, 7073 (1982).
32. P. Ulmer and R. W. Luth, "The Graphite–COH Fluid Equilibrium in P, T, fO_2 Space: An Experimental Determination to 30 kbar and 1600°C," Contrib. Mineral. Petrol. **106**, 265 (1991).
33. I-Ming Chou, "The Oxygen Buffer and Hydrogen Sensor Techniques at Elevated Pressures and Temperatures," in *Hydrothermal Experimental Techniques*, Ed. by G. C. Ulmer and H. L. Barens (Wiley, New York, 1987), pp. 61–99.
34. G. C. Ulmer, D. E. Grandstaff, E. Woermann, *et al.*, "The Redox Stability of Moissanite (SiC) Compared with Metal–Metal Oxide Buffer at 1773 K and at Pressure up to 90 kbar," Neues. Jahrb. Mineral. Abh. **172** (2/3), 279–307 (1998).
35. J. R. Holloway, "Volatile Interactions in Magmas," in *Thermodynamics of Minerals and Melts*, Ed. by R. S. Newton, A. Navrotsky, and B. J. Wood, Adv. Phys. Geochem. **1**, 273–293 (1981).
36. A. A. Ariskin, A. A. Borisov, and G. S. Barmina, "Modeling of the Iron–Silicate Melt Equilibrium in Basaltic Systems," Geokhimiya, No. 9, 1231–1240 (1992).
37. E. Stolper, "The Speciation of Water in Silicate Melts," Geochim. Cosmochim. Acta **46**, 2609–2620 (1982).
38. S. Newman, E. M. Stolper, and S. Epstein, "Measurement of Water in Rhyolitic Glasses: Calibration of an Infrared Spectroscopic Technique," Am. Mineral. **71**, 1527–1541 (1986).
39. E. M. Dianov, M. M. Bubnov, A. N. Gurianov, *et al.*, "Phosphosilicate Glass Optical Fibers: A Promising Material for Raman Lasers," in *Proceedings of ECOC 2000, September 3–7, 2000* (Germany, Munich, 2000), Vol. 3, pp. 135–136.
40. G. Fine and E. Stolper, "The Speciation of Carbon Dioxide in Sodium Aluminosilicate Glasses," Contrib. Mineral. Petrol. **91**, 105–121 (1985).
41. C. G. Pouchert, *The Aldrich Library of Infrared Spectra*, 3rd ed. (Aldrich Chemical Co, 1981).
42. R. Cataliotti and R. N. Jones, "Further Evidence of Fermi Resonance in the C–O Stretching Band of Cyclopentanone," Spectrochim. Acta **27A**, 2011–2013 (1971).
43. B. O. Mysen and D. Virgo, "Volatiles in Silicate Melts at High Pressure and Temperature: 2. Water in Melts along the Join $NaAlO_2$–SiO_2 and a Comparison of Solubility Mechanisms of Water and Auorine," Chem. Geol. **57**, 333–358 (1986).
44. R. W. Luth, B. O. Mysen, and D. Virgo, "Raman Spectroscopic Study of the Solubility Behavior of H_2 in the System Na_2O–Al_2O_3–SiO_2–H_2," Am. Mineral. **72**, 481–486 (1987).
45. D. R. Neuville and B. O. Mysen, "Role of Aluminum in the Silicate Network: In Situ, High-temperature Study of Glasses and Melts on the Joint SiO_2–$NaAlO_2$," Geochim. Cosmochim. Acta **60**, 1727–1737 (1996).
46. B. O. Mysen, "Interaction between Aqueous Fluid and Silicate Melt in the Pressure and Temperature Regime of the Earth's Crust and Upper Mantle," Neues Jahrb. Mineral. Abh. **172** (2/3), 227–244 (1998).
47. A. Debernardi, C. Ulrich, K. Syassen, and M. Cardona, "Raman Linewidths of Optical Phonons in 3C–SiC under Pressure: First-Principles Calculations and Experimental Results," Phys. Rev., No. 10, 6774–6783 (1999).
48. P. Lespade, R. Al-Jishi, and M. S. Dresselhaus, "Model for Raman Scattering from Incompletely Graphitized Carbons," Carbon **5**, 427–431 (1982).
49. J. N. Rouzaud, A. Oberelin, and C. Beny-Baddez, "Carbon Films Structure and Microtexture (Optical and Electron Microscopy, Raman Spectroscopy)," Thin Solid Films **105**, 75–96 (1983).
50. A. V. Sobolev and M. Chaussidon, "H_2O Concentrations in Primary Melts from Supra-Subduction Zones and Mid-Oceanic Ridges: Implications for H_2O Storage and Recycling in the Mantle," Earth Planet. Sci. Lett. **137**, 45–55 (1996).
51. J. R. Holloway, "Graphite–Melt Equilibria during Mantle Melting: Constraints on CO_2 in MORB Magmas and the Carbon Content of the Mantle," Chem. Geol. **147**, 89–97 (1998).